SLAC – PUB – 4196
January 1987
(A)

SURFACE PROPERTIES OF Cr_2O_3 *

R.E. KIRBY, E.L. GARWIN, F.K. KING AND A.R. NYAIESH

Stanford Linear Accelerator Center
Stanford University, Stanford, California, 94305

ABSTRACT

Thin (< 5 nm) air-oxidized Cr layers are deposited on the alumina output windows of radio-frequency klystron tubes to prevent electron multipactor by reducing the secondary electron emission yield of the alumina surface. The top several nanometers of these layers appear to be Cr_2O_3. To compare the measured surface properties of these layers with those of clean stoichiometric Cr_2O_3, quasi-bulk Cr_2O_3 layers were produced by wet-H_2-firing magnetron-deposited Cr films on Cu substrates and characterized by x-ray photoelectron-, Auger electron- and electron energy loss spectra and secondary electron emission yield measurements. Other properties measured were x-ray diffraction structure, sheet resistance and optical reflectivity. In particular, the peak of the secondary electron yield was found to be ~1.7, which is considerably higher than the < 1 yield value reported earlier in the literature.

The Cr_2O_3 Cr 2p XPS core level spectrum was curve-fit using Doniach-Sunjic lineshapes and statistical fitting methods. It is shown that each 2p level is composed of three multiplet-split peaks 1.1 eV apart. In addition the three $2p_{1/2}$ peaks are folded with a $2p_{3/2}$ $3d$-satellite.

Submitted to *Journal of Applied Physics*

* Work supported by the Department of Energy, contract DE – AC03 – 76SF00515.

1. Introduction

A common problem in high-power klystron tube manufacture is breakage of the alumina output window due to electrical breakdown initiated by electron multipactor (resonant multiplication of electrons generated at the high secondary electron yield alumina surface). To prevent the multipactor, the window is usually coated with a thin (1.5-5 nm) layer of a high electrical resistivity (to preclude rf losses), low secondary electron emission (SEE) yield material, such as TiN. In searching for a less stoichiometrically complex system than TiN (whose composition is dependent on N concentration in the gas phase during reactive sputtering or evaporation), we have used air-oxidized Cr layers[1], based on a literature report[2] placing its secondary electron emission coefficient < 1. The SEE yield[1] of these air-oxidized Cr layers is $\sim$1.5, leading to a question of the actual stoichiometry of the layers or of the accuracy of the reported value. Repeating the measurements on bulk Cr_2O_3 was necessary for further investigation.

The SEE yield measurement previously reported[2] was made on layers produced by the air-firing of hydrated CrO_3 on alumina substrates. Using this method, we were also able to produce green insulating layers (presumably Cr_2O_3) on alumina. However, we were unsuccessful in measuring the SEE yield of any of these layers, whose colors ranged from very light green (thin layer) to medium green (thick layer). Cr_2O_3 has quite high resistivity; consequently, a clean layer on alumina simply charges up and repels the primary electron beam during yield measurement. We concluded that the measurement reported[2] was probably done on heavily contaminated samples, whose surface was able toleak off the charge and gave a low yield due to the presence of carbon-containing species. Carbon is known[3] to have a yield < 1.

To reliably produce Cr_2O_3, we deposited 15 nm Cr layers on a conducting substrate, OFHC (oxygen-free high conductivity) Cu, and followed by wet-H_2-firing at 1175K. This thickness of Cr_2O_3 is sufficient to act as bulk material for XPS, AES and SEE yield experiments but thin enough to leak charge to the

Cu substrate. The yield of Cr_2O_3 was found to be higher than that previously reported[2] but low enough to prevent multipactor when used on klystron windows. Although x-ray photoelectron spectroscopy (XPS) results on Cr_2O_3 have been published previously, we nevertheless include both core level and valence band spectra here in order to confirm the chemical nature of our samples as well as their cleanliness. By carefully curve-fitting the XPS Cr 2p levels, the multiplet nature of these peaks is revealed.

2. Experiment

The Cr films were produced by DC magnetron sputtering from an electrochemically deposited 99.99% pure Cr target. The deposition conditions were: 5 x 10^{-3} Torr Ar at 0.2A discharge current, 300V applied voltage, 0.1 m target-substrate separation and a deposition rate of 0.35 nm/sec. Thickness was monitored using an AT-cut quartz crystal and oscillator. The Cr films were converted to Cr_2O_3 by firing in wet-H_2 at 1175K for 30 minutes. To confirm that the films were indeed Cr_2O_3, a thicker (2.4 μm) film was produced on OFHC copper, fired and subsequently analyzed by x-ray diffraction. The intensities and d-spacings are given in Table I. These were compared to chromium-based powder patterns found in the ASTM Powder Diffraction File[4]. Only four strong lines could be identified because of the thinness of the sample; however, the d-spacings are in excellent agreement with the file identification for chromium (III) oxide (Cr_2O_3). The intensities are mismatched because of the apparently strong preferred orientation of the deposited sample versus the powdered sample used for the reference file.

Sheet resistance measurements were made via standard four-point probe at room temperature. The surface analytical instrumentation (yield, XPS, Auger electron spectroscopy (AES) and electron energy loss spectroscopy (ELS)) is described in detail in references 1 and 5. Those measurements were made at room temperature as well. The binding energy references for XPS are Ag

$3d_{5/2}$ = 368.2 eV and the Pd Fermi edge = 0 eV. Optical reflectivity measurements were made using an IBM Model 9430 spectrophotometer equipped with deuterium and tungsten lamps.

3. Results and Discussion

I. SHEET RESISTANCE

Additional Cr_2O_3 layers were produced by the method described above on 99.6% pure alumina substrates (.15 μm surface finish) for the measurement of sheet resistance and optical reflectivity. The resistance measurements were made for a variety of Cr post-deposition treatments that are typically encountered in klystron tube manufacture and to which Cr_2O_3-coated klystron windows are subjected. These results are given in Table II. In particular, the Cr_2O_3 (wet-H_2-fired Cr) layers show the resistance expected for a completely converted Cr film, i.e., $>10^{11}$ Ω/square. Additionally, these Cr_2O_3 layers on alumina show a very light green sheen typical of thin layers of this oxide. The as-deposited Cr films are light gray in color on Al_2O_3.

One notes from Table II that there is a considerable variation in sheet resistance for the baked samples. The oxidized and baked surface has some Cr metal underlayer[1] and the surface Cr_2O_3 over the Cr may be punctured through to remaining metal underlayer by the four-point probe, thereby explaining the low sheet resistance values for some of the baked samples.

II. OPTICAL REFLECTIVITY

Optical reflectivity spectra (Figure 1) were measured on samples from the same Cr depositions and firings used for samples in the sheet resistance measurements. Four absorptions (250, 355, 460 and 600 nm) are visible in the spectrum of wet-H_2-fired Cr in Figure 1. These absorptions are expected for electronic transitions of a Cr^{3+} ion in an octahedral crystal field and have been measured before in Cr_2O_3[6–10]. Three of these absorptions (355, 460, and 600 nm) are

spin-allowed *d-d* transitions while the fourth (250 nm) is apparently a charge transfer from ligand to metal-ion, although this last appears to also be a feature (Figure 1) of the uncoated alumina substrate as well.

The spectrum of air-exposed 15 nm Cr-coated alumina is very different from that of the wet-H_2-fired Cr layer, although one can see the incipient absorptions, or possibly the substrate, appearing at shorter wavelength. Our earlier study[1] showed that only a few nanometers of this layer is Cr_2O_3, so it is not surprising that the optical spectra do not reveal a strong Cr_2O_3 spectrum for the air-oxidized surface.

III. SEE YIELD

To measure the yield of Cr_2O_3, a clean, stoichiometric surface is required. The samples produced by wet-H_2-firing of oxidized Cr films on OHFC Cu are surface-carbon-contaminated, as determined by AES. Ion sputter cleaning is typically used in such cases. However, for many metal oxides, ion bombardment results in reduction of the surface[11], particularly at normal ion beam incidence[3,12]. Oxides with free energies of formation above 118 kcal/mole are stable against ion bombardment at room temperature[11], unless there is a higher oxide with a stable intermediate. The free energy of Cr_2O_3 is 250 kcal/mole and it has no stable intermediate, therefore, it is unlikely to decompose under bombardment. Previous work done on the ion bombardment of metal oxides used AES[12] and XPS[11,13] to test for ion-induced oxide reduction. Our experience, however, is that the SEE yield is more sensitive to surface changes, chemical or structural, than is AES or XPS.

If the Cr_2O_3 surface is reduced by bombardment, then exposure to air should restore the oxide[1,14]. Following air exposure, there will also be excess water and hydrocarbons adsorbed on the Cr_2O_3 surface. That layer can be removed by heating well below the temperature at which the oxide might be decomposed. Sputtering our sample with a total dose of 10^{15} ions/cm^2, 1.5 keV energy was sufficient to render the surface carbon-free. The sample was then exposed to

room air for one hour, followed by heating at 825K in vacuum for two hours to remove any excess water vapor or hydrocarbons. In Figures 2-7, the yield, AES, XPS and ELS results are presented.

The AES, ELS, XPS core level and XPS valence band spectra (Figures 3-7) are virtually identical for the sputtered, air-exposed and heated cases. We present the heated case since we believe this, most likely, to be the clean, stoichiometric surface. The yields measured (Figure 2) for the bombarded, air-exposed and heated surfaces are different for the three cases, however, and are 1.67, 1.85 and 1.75, respectively. The heated value is about 15% higher than that for air-oxidized and heated 14 nm Cr films on alumina studied earlier[1]. The difference seems to be that the actual Cr_2O_3 layer thickness in that study was 1.3 nm. Therefore, there was a reduction of the SEE yield due to the presence of lower yield underlying Cr metal. Trapping of secondaries due to substrate roughness[3] may also effectively reduce the yield in the alumina substrate case.

IV. AES

The Auger electron spectrum of the heated Cr_2O_3 layer on Cu is presented in Figure 3. Because the oxygen KLL transitions occur within the spread of Cr LMM transitions, an attempt was not made to compare this spectrum to Cr. The N(E) spectrum does not appear to have been published previously, possibly because of this difficulty. The higher kinetic energy portion of the spectrum (800-1000 eV range) does not show any Cu peaks due to the substrate, indicating that the Cr_2O_3 XPS valence band spectrum (whose photoelectrons have similar kinetic energy, and hence, similar escape depth) presented below does not suffer from substrate interference.

V. XPS CORE LEVELS

Figures 4 and 5 show the Cr 2p and O 1s core levels for the heated Cr_2O_3 layer on Cu. These Cr core levels are quite asymmetrical (discussed below), however, the peak centroid and area have been determined from lineshape fits and compared to the literature. The binding energy positions of the Cr $2p_{3/2}$

level = 577.0 eV and O 1s level = 530.8 eV are in good agreement with literature values of 576.8 eV[16] and 530.6 eV[17], respectively, when the binding energy references of the literature values are brought into agreement with those used in this work. The Cr/O peak areal ratio for the Cr $2p_{3/2}$ and O 1s peaks is 1.54. Using published[18] XPS sensitivity factors of 1.5 for Cr and 0.66 for O gives an atomic ratio of Cr/O=0.68, comfortingly near the theoretical Cr_2O_3 atomic ratio of 0.67.

The peak asymmetry evident in the Cr 2p data has been observed before in transition metal compounds and commented on as being possibly due to multiplet splitting[16,19], $3d$ satellites[20], or mixed valencies[21]. Each of these possibilities are discussed in turn.

Multiplet splitting can be observed readily in the 3s levels of Mn compounds where the separation between the multiplet lines is often greater than 10 eV[22]. For 2p states, however, the splitting is apparently much smaller and may not be experimentally resolvable because of overlap of the multiplet-split peaks. This effect could account for the observed experimental asymmetry in the Cr 2p data. Presumably, that asymmetry should be identical for both of the spin-orbit-split 2p levels - but is not, apparently because of other contributions to the lineshape.

Satellites have been observed in Cr_2O_3 spectra where screening of the $3d$ ion results in satellite lines about 11 eV B.E. above the parent 2p lines[20]. The observed asymmetry in our Cr 2p data could be due to a satellite of the $2p_{3/2}$ line coinciding with the $2p_{1/2}$ line. We have, in fact, measured a $2p_{1/2}$ satellite at 11.2 eV B.E. above the $2p_{1/2}$ core line having 15% of the areal intensity of the $2p_{1/2}$ peak.

Cr_2O_3 is not a mixed valency compound so the observed asymmetry is not due to that reason. Also, the evidence presented in earlier sections supports our contention that only one oxide state of Cr is present. We have curve-fitted the experimental data of Figure 4 using a procedure previously described[1]. The theoretical peaks used in the fit have a Doniach-Sunjic lineshape characterized by

parameters such as half width, energy position, asymmetry, phonon broadening and background. The goodness-of-fit is determined by calculating the reduced chi-squared (χ^2) value[23] for the theoretical fit to the data, an excellent fit giving a value equal to one and good fits giving a value around two. The values of these various parameters for the fits of Figure 4 are listed in Table III.

Because of the presence of the $2p_{3/2}$ satellite under the $2p_{1/2}$ peak, the fit requires that, if n peaks are used for the $2p_{3/2}$ peak fit, then n + 1 will be needed for the $2p_{1/2}$ peak. In fact, it was found that a minimum n for a good fit is three. That number also coincides with the expected number of multiplet-split levels[19]. After fitting the $2p_{3/2}$ with three peaks, we placed 15% of the intensity of these respective peaks at 11.2 eV higher binding energy than each of them, their sum total then becoming the $2p_{3/2}$ satellite. The fitting program was then allowed to add three additional peaks to this and fit the $2p_{1/2}$ intensity, subject to the constraint that the energy separation between these additional three peaks be the same as that between the three $2p_{3/2}$ peaks. That constraint simply reflects the constancy of the spin-orbit-splitting between the $2p_{3/2}$ and $2p_{1/2}$ levels.

The fitting was done in two intervals, 573-582 eV and 584-591 eV because the lineshape of the $2p_{3/2}$ satellite is the same as that of the $2p_{3/2}$ peak and, therefore, the $2p_{3/2}$ peak had to be fit first in order to obtain the shape of the satellite. Several points can be noted. First, the $2p_{3/2}$ fit is somewhat better than that of the $2p_{1/2}$. All parameters were allowed to vary when fitting the $2p_{3/2}$ peak whereas the number of peaks and their energy positions were fixed for the $2p_{1/2}$ fit so that only the intensity of the three multiplet-split peaks could vary. It is therefore not surprising that the fit is poorer. If more peaks had been used in the $2p_{3/2}$ fit then very probably the $2p_{1/2}$ peak fit would improve. However, that would be an unphysical result because of the requirement of no more than three multiplet-split $2p_{1/2}$ levels[19]. Second, the 15% areal intensity used for the $2p_{3/2}$ satellite is a minimum area and could possibly be somewhat higher. This happens because the $2p_{3/2}$ satellite cannot contribute to the $2p_{1/2}$ satellite and the 15% figure was determined by dividing the experimental $2p_{1/2}$ satellite area

(not shown) by the total $2p_{1/2}$ peak area. Therefore 15% is an underestimate but is probably near the correct value. A re-fit of the data using either a 20% or a 10% contribution for the $2p_{3/2}$ satellite gives a χ^2 value which is larger than the 15% value, thereby supporting this contention. Third, the intensity ratios between the pairs of spin-orbit-split 2p peaks is not constant. That also suggests that some further contribution to the $2p_{1/2}$ intensity is needed.

To our knowledge, the 2p multiplet structure of Cr_2O_3 has not been calculated quantitatively, so a direct comparison with theory is not presently possible. Qualitatively[19], about equal separations in energy are expected between the three multiplet-split components of the $2p_{3/2}$ level and that is what we achieve ($\sim$1.1 ev) for a good fit.

VI. XPS VALENCE BAND

The XPS valence band of Cr_2O_3 has been extensively studied[16,20,24–26] because of interest in $3d$ hole screening in transition-series insulators. Figure 6 shows the band for the heated Cr_2O_3 layer on Cu. The main features are a Cr 3d line (B.E.=2.7eV), a broad O 2p band (B.E.=7.1 eV), and a Mg $K\alpha_{3,4}$ x-ray satellite (B.E.=14.3 eV) of the O 2s line. An expected[20] weak Cr 3d satellite at B.E. $\sim$ 14.8 eV is obscured by the presence of the x-ray satellite. The inelastic background in our spectrum appears to be somewhat lower than in published spectra and may explain why our spectrum shows a larger Cr 3d/O 2p ratio. The reason for the reduced background is not known. The energy dependence of the instrument transmission is not a factor over such a small energy range; however, the presence of an amorphous contamination layer would give increased inelastic scattering. The most recent published spectrum[20] does show lower background and a larger Cr 3d/O 2p ratio but the surface cleanliness was unconfirmed by XPS or AES (or at least not reported in print).

VII. ELS

There appears to be only one previously published[27] ELS spectrum of Cr_2O_3 (prepared by heating Cr(110) in 10^{-6} torr O_2 at 775K-875K for five minutes).

Our spectrum for heated Cr_2O_3 on Cu (Figure 7) is very similar, particularly in the reproduction of a large number of features unique to Cr_2O_3, as opposed to oxygen-covered Cr. Interpretation of these peaks may be found in reference 27. The bulk plasmon (~24 eV loss) appears more developed in our spectrum, possibly due to a thicker oxide layer than in reference 27. Other than that, the spectrum does not warrant further comment.

4. Conclusion

The results presented above show that wet-H_2-firing of Cr reliably produces Cr_2O_3 and that the SEE yield of the clean Cr_2O_3 surface is around 1.7. The use of Cr_2O_3 layers for suppressing secondary electron emission from insulators is technically appealing; several nanometers of Cr are deposited and then air exposed to form the Cr_2O_3 layer. The high resistivity of this layer makes it ideal for uses where the suppression of radio-frequency losses is important. Stoichiometry is assured – Cr oxidizes in air or oxygen at room temperature and pressure to only one oxide state. It remains stable, even in vacuum, to at least 825K[1].

Elucidation of the multiplet structure of the XPS Cr 2p levels in Cr_2O_3, although not technically important, is nevertheless of interest. It is generally accepted that in order to resolve overlapping peaks, higher resolution instruments need be used. In particular, monochromatization of the x-ray source is usually the first enhancement made. That would, in our case, reduce the FWHM of the total instrument response function (made up of the x-ray linewidth and the analyzer resolution function) from 0.75 eV to about 0.40 eV. Is that sufficient by itself to deduce the number of peaks, and their positions, that make up the Cr $2p_{3/2}$ level, for example?

To answer this question, we have taken the three theoretical Doniach-Sunjic lineshapes used to curve fit the Cr $2p_{3/2}$ level in Figure 4 and folded them with an instrument response having a FWHM of 0.40 eV. The result is shown in Figure 8. Clearly, an examination of such data without statistical curve fitting would still

not reveal the number of peaks present (or their positions). In some cases where experimental peak separations are larger, or the natural linewidths of the peaks are narrower, monochromatization is the answer, provided space is available on the experimental system for the addition of an x-ray monochromator. Curve fitting, though, is likely to be more cost effective, particularly when the loss of intensity of non-monochromatized versus monochromatized sources is taken into account.

5. References

1. A.R. Nyaiesh, E.L. Garwin, F.K. King and R.E. Kirby, J. Vac. Sci. Technol. 4, 2356 (1986).
2. T.S. Sudarshan and J.D. Cross, IEEE Trans. Elec. Insul. EI-11, 32 (1976).
3. E.L. Garwin, E.W. Hoyt, R.E. Kirby and T. Momose, J. Appl. Phys. 59, 3245 (1986).
4. ASTM Powder Diffraction File (Joint Committee on Powder Diffraction Standards, Swathorne, Pennsylvania, 1980).
5. E.L. Garwin, F. K. King, R.E. Kirby and O. Aita, J. Appl. Phys. 61, No. 2 (1987).
6. I. Fanderlik, Optical Properties of Glass, Elsevier, Amsterdam (1983).
7. B. Karlsson and C.G. Ribbing, J. Appl. Phys. 53, 6340 (1982).
8. T.I.Y. Allos, R.R. Birss, M.R. Parker, E. Ellis and D.W. Johnson, Solid State Comm. 24, 129 (1977).
9. J.C.C. Fan, Thin Solid Films 54, 139 (1978).
10. G.V. Subba Rao, C.N.R. Rao and J.R. Ferraro, Appl. Spectroscopy 24, 436 (1970).
11. K.S. Kim, W.E. Baitinger, J.W. Amy and N. Winograd, J. Electron Spec. Rel. Phenom. 5, 351 (1974).
12. B. Bartezky and E. Taglauer, Surface Sci. 162, 996 (1985).
13. N.S. McIntyre and F.W. Stanchell, J. Vac. Sci. Technol. 16, 798 (1979).
14. F. Watari, Surface Sci. 110, 111 (1981).
15. J.C. Fuggle, in Electron Spectroscopy: Theory, Techniques and Applications, C.R. Brundle, Editor, Academic Press, New York (1981).
16. I. Ikemoto, K. Ishii, S. Kinoshita, H. Kuroda, M.A. Alario Franco and J.M. Thomas, J. Sol. State Chem. 17, 425 (1976).

17. G. Gewinner, J.C. Pruchetti, A. Jaegle and A. Kalt, Surface Science 78, 439 (1978).

18. C.D. Wagner, J. Electron. Spect. Rel. Phenom. 32, 99 (1983).

19. G.C. Allen and P.M. Tucker, Inorg. Chim. Acta 16, 41 (1976).

20. B.W. Veal and A.P. Paulikas, Phys. Rev. B 31, 5399 (1985).

21. C.N.R. Rao, D.D. Sarma, S. Vasudevan and M.S. Hegde, Proc. R. Soc. Lond. A367, 239 (1979).

22. D.A. Shirley, Topics in Applied Physics 26, 165 (1978).

23. For a discussion of reduced χ^2 see, for example, P.R. Bevington, Data Reduction and Error Analysis for the Physical Sciences, McGraw-Hill, New York (1969), p. 187.

24. G.K. Wertheim, H.J. Guggenheim and S. Hüfner, Phys. Rev. Lett. 30, 1050 (1973).

25. W.Y. Howng and R.J. Thorn, Phys. Status Solidi 41, 75 (1980).

26. F. Werfel and O. Brümmer, Physica Scripta 28, 92 (1983).

27. Y. Sakisaka, H. Kato and M. Ouchi, Surface Sci. 120, 150 (1982).

Table I. X-Ray Diffraction Results

<hkl> Reflection	Reference[a] d-spacing (nm)	Reference[a] I/I_0	Measured d-spacing (nm)	Measured I/I_0
<110>	0.2480	.95	0.2481	.04
<024>	0.1816	.40	0.1810	.12
<300>	0.1431	.40	0.1439	1
<226>	0.1087	.18	0.1089	.17

Sample: Wet-H_2 fired (1175K, 18 hours) Cr film (2.4 μm thickness) deposited on polished OFHC copper substrate.

[a]Reference 4.

Table II. Sheet Resistance (Ω/Square) Measurement 15nm Cr on Alumina

Sample[a] No.	1[b]	2
Deposited and exposed to air	$(1.1\text{-}1.7)\times10^3$	4.1×10^2
Deposited, exposed to air and baked in vacuo to 823K, 170 hours	5.3×10^3 to 4.2×10^{10}	1.6×10^3
Deposited, exposed to air and air-fired, 1275K, 10 min.	$(0.8\text{-}6.7)\times10^{10}$	—
Deposited, exposed to air and wet-H_2 fired, 1175K, 30 min.	$>10^{11}$	$>10^{11}$

[a]Each sample was divided in pieces following deposition.

[b]This sample was measured in five different places on its surface.

Table III. Cr 2p Fit Peak Parameters[a]

Peak No.	Level	Position (eV)	Height[b]	Asymmetry	Half-Width (eV)
1	$2p_{3/2}$	576.3	1.00	0.133	1.6
2	$2p_{3/2}$	577.4	0.72	0.077	1.5
3	$2p_{3/2}$	578.6	0.25	0.030	1.9
4	$2p_{1/2}$	585.4	0.27	0.133	1.6
5	$2p_{1/2}$	586.5	0.40	0.077	1.5
6	$2p_{1/2}$	587.7	0.15	0.030	1.9
7	15% of the sum of 1,2 and 3 peak areas placed at 11.2 eV higher binding energy				

[a] These parameters refer to Figure 4 and characterize Doniach-Sunjic lineshapes.

[b] Heights are normalized to the peak No. 1 height.

Figure Captions

1. Measured optical reflectivity spectra of an uncoated alumina substrate (—), air-exposed 15 nm Cr-coated alumina (- - -) and wet-H_2-fired 15 nm Cr-coated alumina (- · -). The arrows mark absorptions discussed in the text.

2. Total secondary electron emission (SEE) yield for wet-H_2-fired 15 nm Cr-coated alumina. After 10^{15} ions/cm^2, 1500 eV (- · -); following air exposure, 1 hour at 1 atmosphere pressure (- - -); after 825K anneal, 2 hours (—). Primary electron beam exposure during measurement was 5 x 10^{15} electrons/cm^2/curve (4.9 keV, 2 nA beam).

3. Auger electron spectrum of wet-H_2-fired 15 nm Cr-coated OFHC Cu after ion bombardment, air exposure and heating to 825K for 2 hours. N(E) data was collected in pulse count mode and smoothed ten times using a 5-point polynominal. N'(E) data is the mathematical differential of the smoothed N(E) data. Auger transition assignments are taken from reference 15.

4. XPS Cr 2p levels for sample of Figure 3. Binding energy of the centroid of Cr $2p_{3/2}$=577.0 eV. The x-ray source was non-monochromatized Mg K$\alpha_{1,2}$ (hν=1253.6 eV). The total instrument response (x-ray linewidth plus analyzer resolution) is 0.75 eV FWHM. The experimental data are the upper dots and the total curve fit is the solid line through these data points. The fitting procedure is discussed in the text and the component parameters for the fitting peaks 1-6 are found in Table III. Peak 7 is the $2p_{3/2}$ satellite. χ^2=2.49 for $2p_{3/2}$ and χ^2=4.44 for $2p_{1/2}$ total fits.

5. XPS O 1s core level for sample of Figure 3. Binding energy = 530.8 eV.

6. XPS valence band for sample of Figure 3. Main features are the 3d level (1), O 2p level (2) and an O 2s x-ray satellite (3). The energy reference is the Pd Fermi edge at B.E. = 0.

7. ELS spectrum for sample of Figure 3. Primary energy (Ep)=300 eV, at 19.5° from normal incidence. Indicated features (arrows) coincide with similar features in reference 27.

8. XPS Cr $2p_{3/2}$ level. Dashed curve is a re-fit using the Doniach-Sunjic lineshapes determined in Figure 4 with a pseudo-monochromatized total instrument response function of 0.40 eV FWHM. The solid curve is the fit from Figure 4 using a non-monochromatized response of 0.75 eV FWHM, for comparison. The inelastic background normally added to these fits, and used in Figure 4, has been omitted here for clarity.

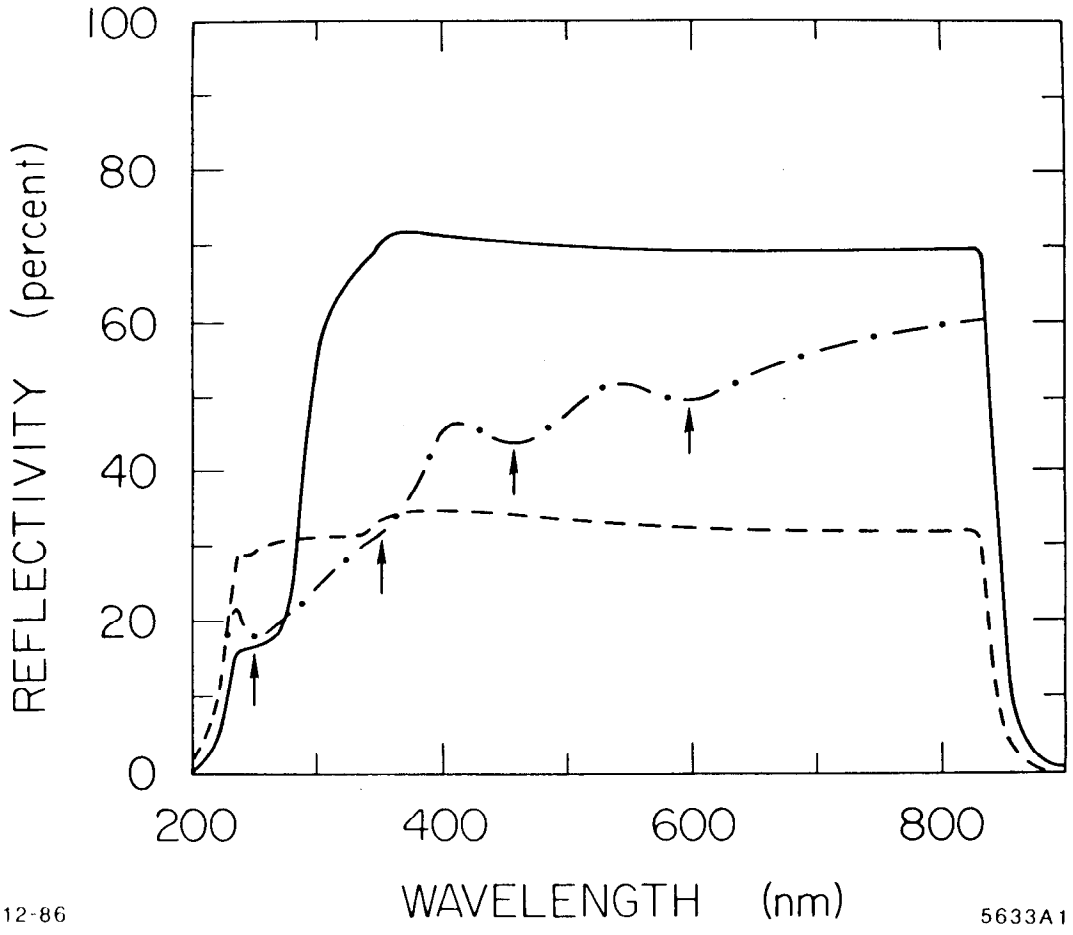
100
80
60
40
20
0
REFLECTIVITY (percent)
200
400
600
800
WAVELENGTH (nm)
12-86
5633A1

Fig. 1

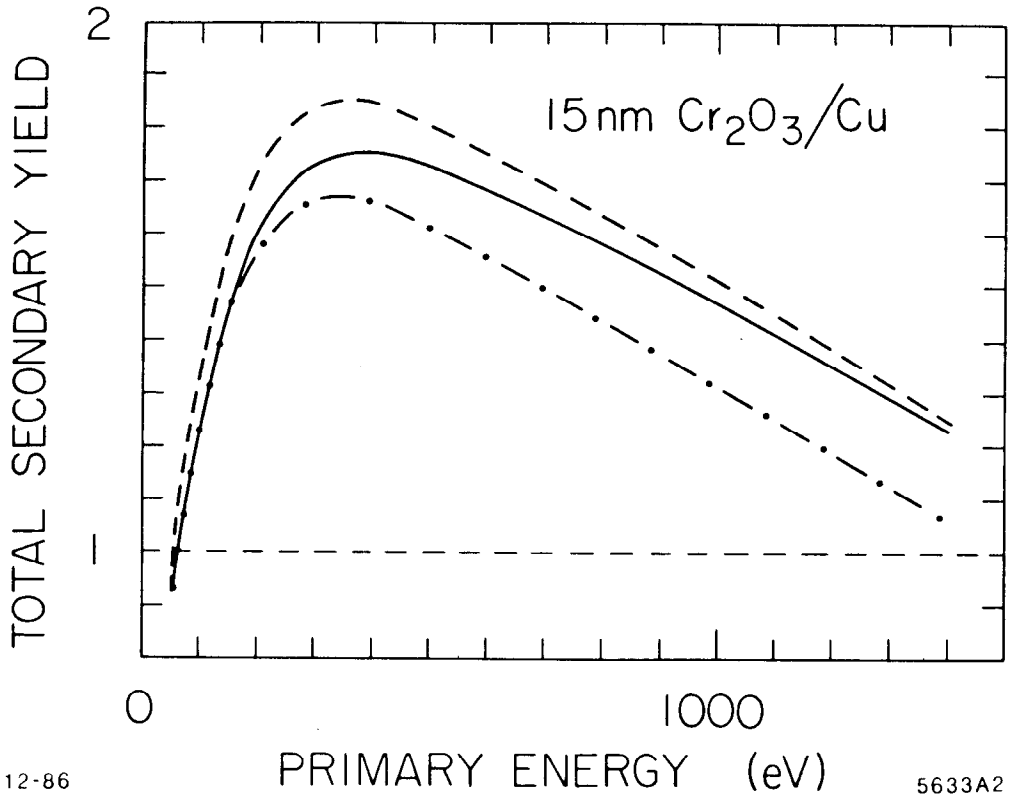
2
1
TOTAL SECONDARY YIELD
15nm Cr_2O_3/Cu
0
1000
PRIMARY ENERGY (eV)
12-86
5633A2

Fig. 2

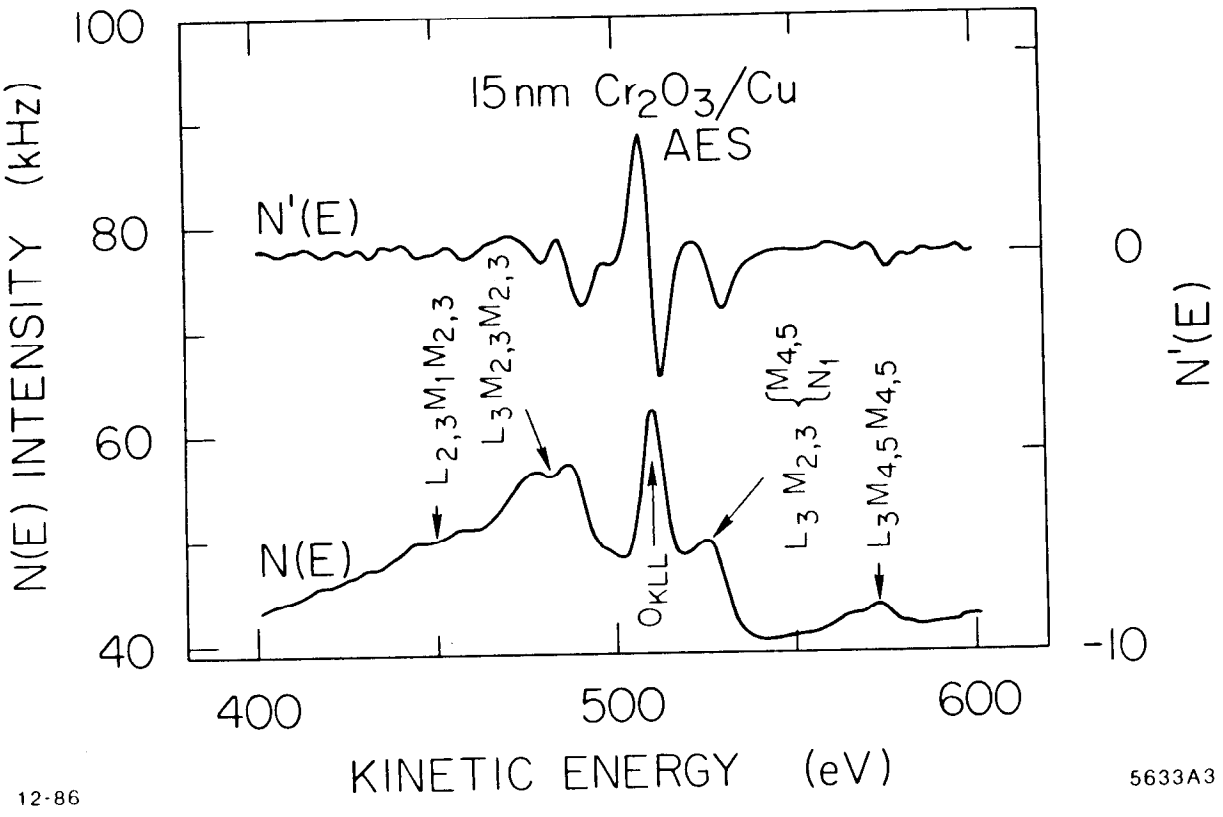
15nm Cr_2O_3/Cu
AES
N'(E)
N(E)
$L_{2,3}M_1M_{2,3}$
$L_3M_{2,3}M_{2,3}$
$L_3M_{2,3}$ $\{^{M_{4,5}}_{N_1}$
$L_3M_{4,5}M_{4,5}$
O_{KLL}
100
80
60
40
0
-10
400
500
600
N(E) INTENSITY (kHz)
N'(E)
KINETIC ENERGY (eV)
12-86
5633A3

Fig. 3

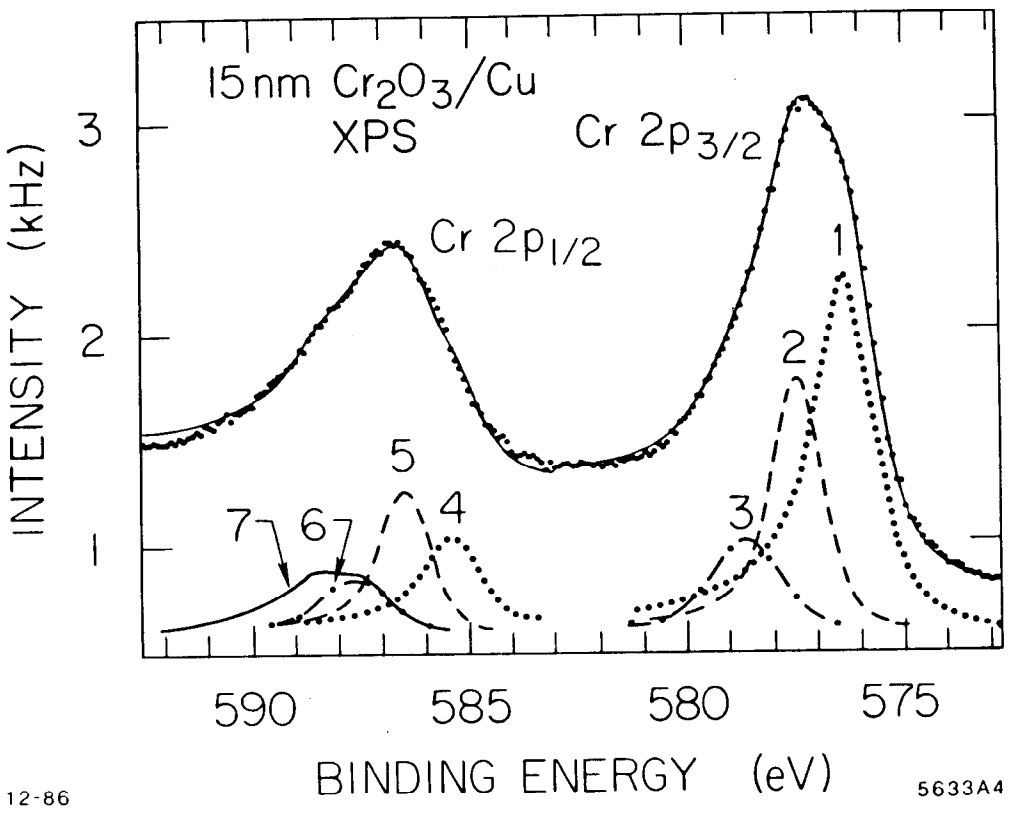
15nm Cr_2O_3/Cu
XPS
Cr $2p_{3/2}$
Cr $2p_{1/2}$
1
2
3
4
5
6
7
INTENSITY (kHz)
3
2
1
590
585
580
575
BINDING ENERGY (eV)
12-86
5633A4

Fig. 4

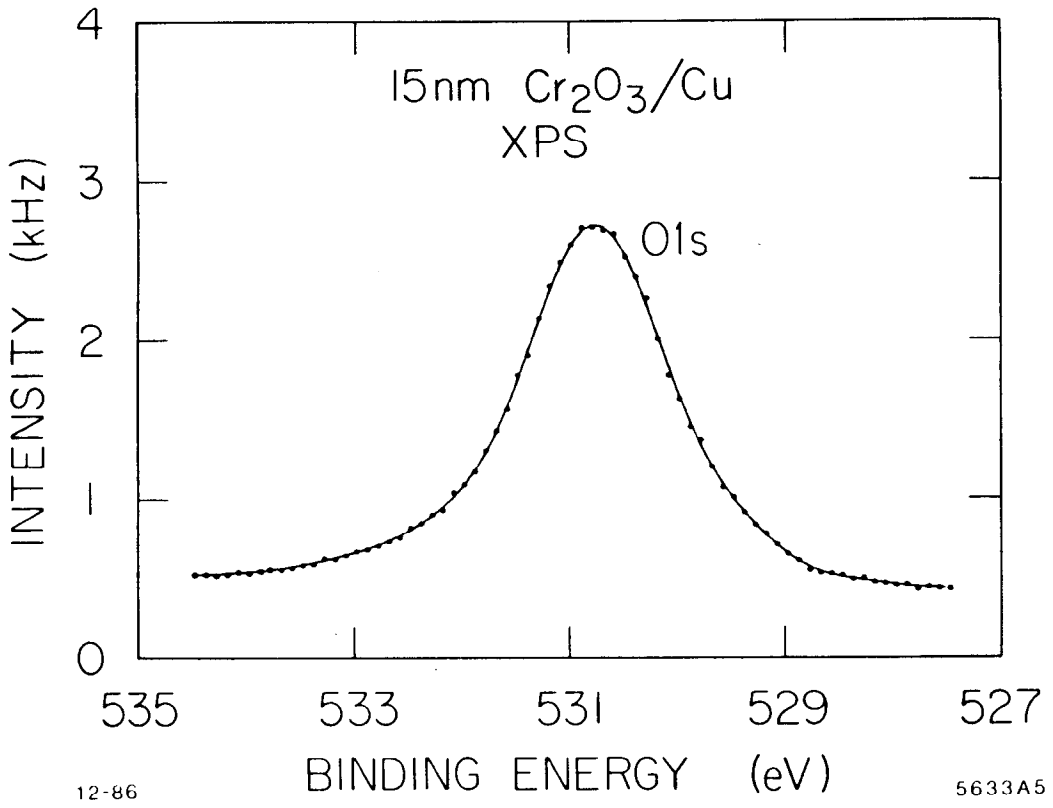
15nm Cr_2O_3/Cu
XPS
O1s
INTENSITY (kHz)
4
3
2
1
0
535
533
531
529
527
BINDING ENERGY (eV)
12-86
5633A5

Fig. 5

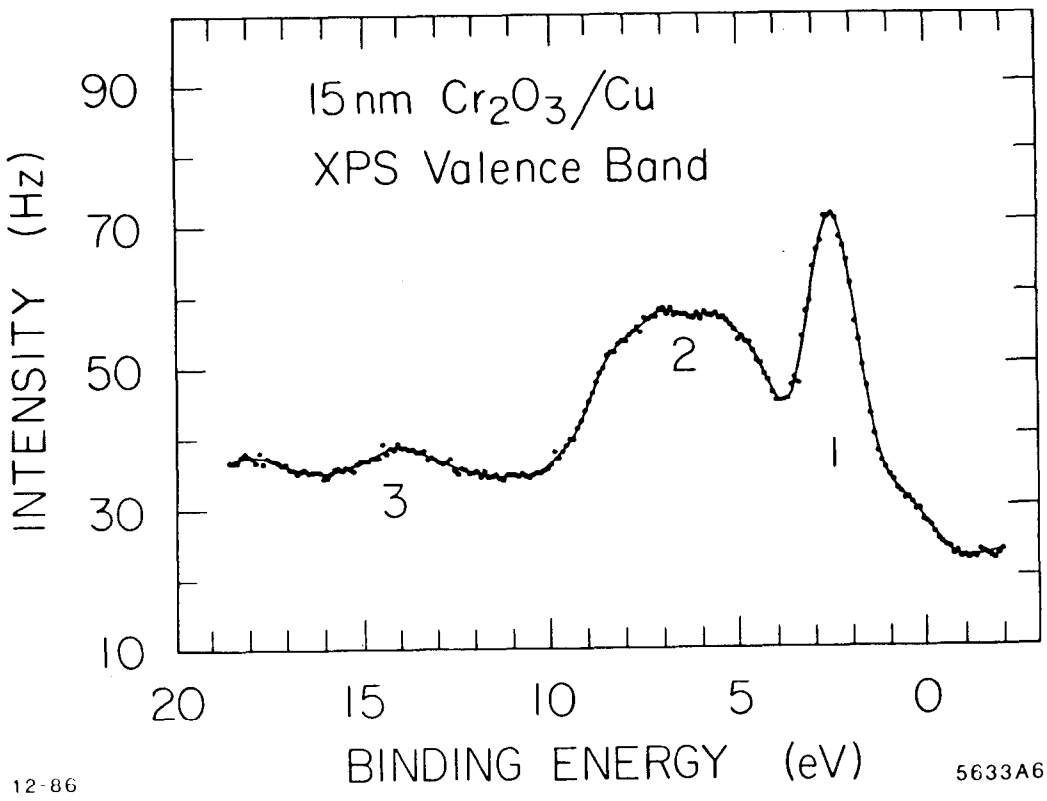
15 nm Cr_2O_3/Cu
XPS Valence Band
INTENSITY (Hz)
90
70
50
30
10
20
15
10
5
0
BINDING ENERGY (eV)
1
2
3
12-86
5633A6

Fig. 6

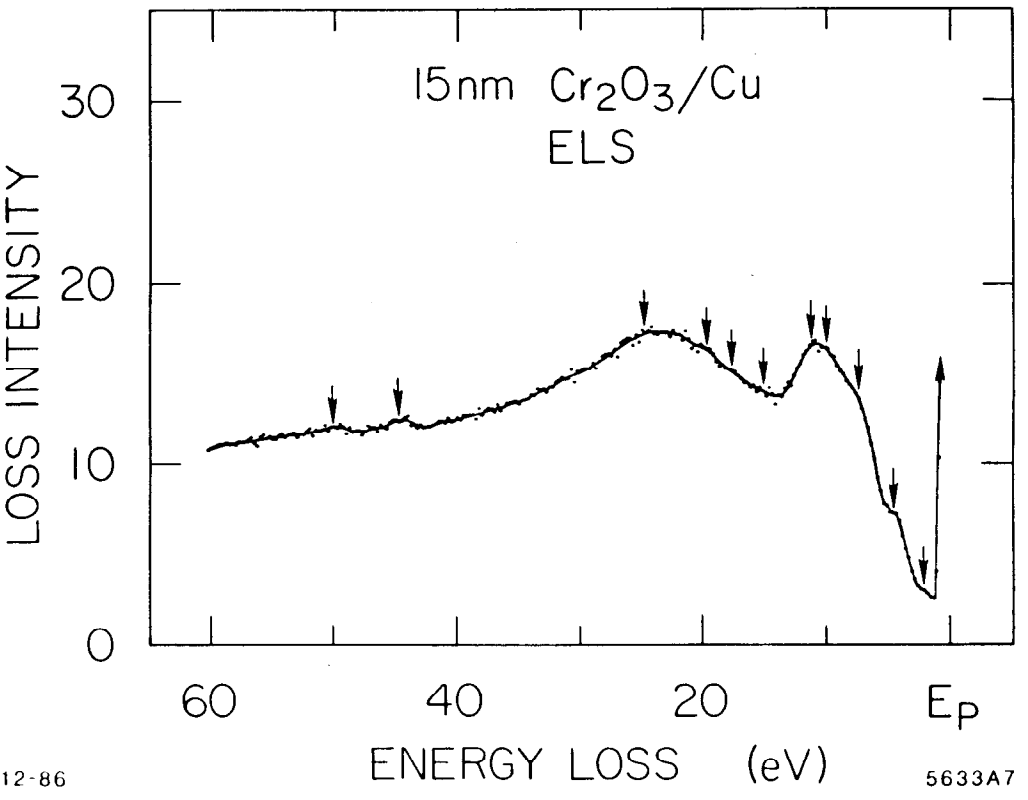
15nm Cr_2O_3/Cu
ELS
LOSS INTENSITY
30
20
10
0
60
40
20
E_P
ENERGY LOSS (eV)
12-86
5633A7

Fig. 7

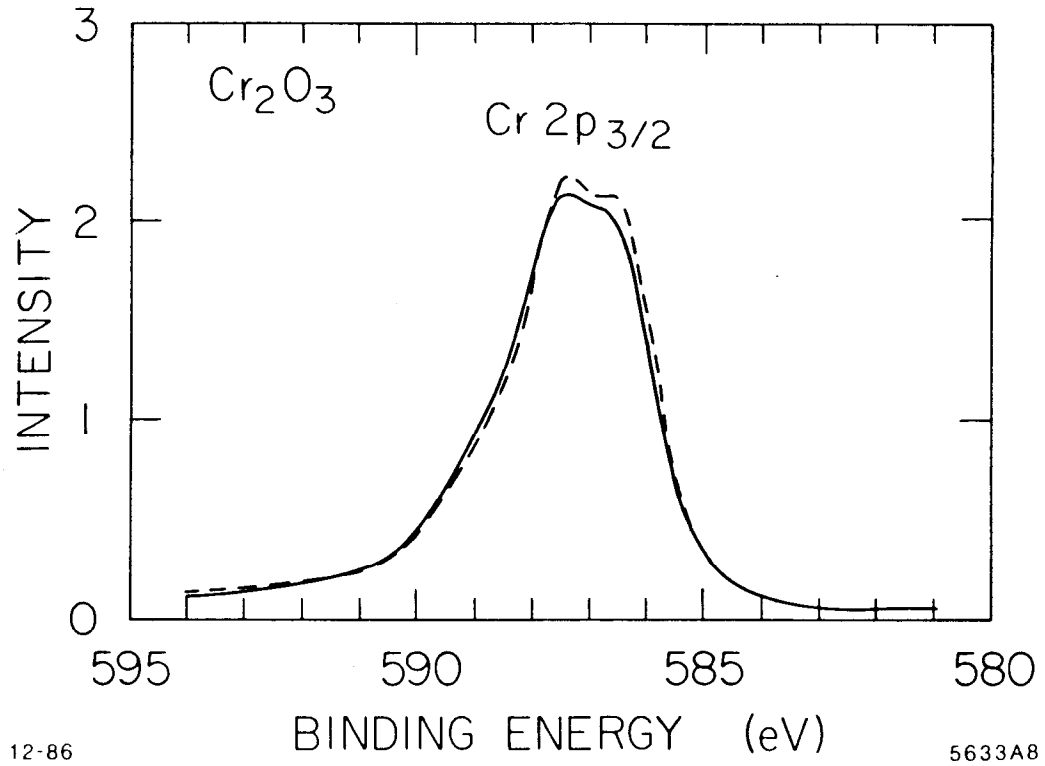
3
2
1
0
INTENSITY
Cr_2O_3
Cr $2p_{3/2}$
595
590
585
580
BINDING ENERGY (eV)
12-86
5633A8

Fig. 8